

Experimental Self-Characterization of Quantum Measurements

Aonan Zhang^{1,2,‡}, Jie Xie^{1,2,‡}, Huichao Xu^{1,2}, Kaimin Zheng^{1,2}, Han Zhang^{1,2}, Yiu-Tung Poon^{3,4,5},
Vlatko Vedral^{6,7,*} and Lijian Zhang^{1,2,†}

¹National Laboratory of Solid State Microstructures, Key Laboratory of Intelligent Optical Sensing and Manipulation (Ministry of Education), College of Engineering and Applied Sciences and School of Physics, Nanjing University, Nanjing 210093, China

²Collaborative Innovation Center of Advanced Microstructures, Nanjing University, Nanjing 210093, China

³Department of Mathematics, Iowa State University, Ames, Iowa 50011, USA

⁴Shenzhen Institute for Quantum Science and Engineering, Southern University of Science and Technology, Shenzhen 518055, China

⁵Center for Quantum Computing, Peng Cheng Laboratory, Shenzhen, 518055, China

⁶Atomic and Laser Physics, Clarendon Laboratory, University of Oxford, Parks Road, Oxford OX13PU, United Kingdom

⁷Centre for Quantum Technologies, National University of Singapore, 3 Science Drive 2, 117543, Singapore



(Received 9 July 2019; published 28 January 2020)

The accurate and reliable description of measurement devices is a central problem in both observing uniquely nonclassical behaviors and realizing quantum technologies from powerful computing to precision metrology. To date quantum tomography is the prevalent tool to characterize quantum detectors. However, such a characterization relies on accurately characterized probe states, rendering reliability of the characterization lost in circular argument. Here we report a self-characterization method of quantum measurements based on reconstructing the response range—the entirety of attainable measurement outcomes, eliminating the reliance on known states. We characterize two representative measurements implemented with photonic setups and obtain fidelities above 99.99% with the conventional tomographic reconstructions. This initiates range-based techniques in characterizing quantum systems and foreshadows novel device-independent protocols of quantum information applications.

DOI: 10.1103/PhysRevLett.124.040402

The information of any quantum system we can acquire, manipulate, and transmit is finally revealed by quantum measurements. As the measuring devices become increasingly sophisticated, the implementations of both tests of quantum theories and quantum information applications [1–4] require experimental calibration and certification of a measurement apparatus, which is normally achieved by recording the measurement outcomes on probe states. In the principle of quantum mechanics, the operation of a quantum measurement on quantum states complies with Born’s rule $p_k^{(j)} = \text{Tr}(\rho^{(j)}\pi_k)$, $k = 0, 1, \dots, n - 1$. Here $\{\rho^{(j)}\}$ represents quantum states described by density matrices and $\{\pi_k\}$ is the positive-operator-valued measure (POVM) of a quantum measurement with n outcomes. This formula describes the measurement as a mapping from the state space of quantum systems $\{\rho | \rho \geq 0, \text{Tr}(\rho) = 1\}$ to the classically accessible detector outcomes represented in the probability space $\{(p_0, p_1, \dots, p_{n-1})\}$, thus enabling us to predict the measurement results and also perform the inverse, i.e., to identify the measurement operators in accordance with observed results. To do this, one could probe the measurement device by identical copies of a set of known states, and then find the POVM $\{\pi_k\}$ closest to the observed results, for example, by optimizing the least square function,

$$\min \sum_{j,k} [p_k^{(j)} - \text{Tr}(\rho^{(j)}\pi_k)]^2, \quad (1)$$

under the physical constraint $\pi_k \geq 0$ and $\sum \pi_k = I$, where I denotes the identity operator. This method, known as quantum detector tomography (QDT), has been suggested as the standard tool of characterizing quantum measurements [5–8].

Despite the success of QDT, an unavoidable issue arises in real-world applications, that is, the accuracy of the tomography results relies on precisely calibrated probe states [see Fig. 1(a)]. Conversely, to calibrate the source for probe states one requires a convincing measurement device, which forms a fundamental loop paradox. Efforts have been made to develop improved tomography techniques such as self-calibrating tomography, that relaxes partial knowledge in the state or the measurement side [9,10]. On the other hand, in certain cases quantum states and measurements can be “self-tested” in a device-independent (DI) way [11–14], i.e., without assuming the internal workings of the apparatus used. These self-testing methods originated from ensuring secure cryptography [11] and were then utilized to bound dimensionality [15,16], generate random numbers [17–19], and verify quantum computers [20]. In this line, DI tests are typically based on a witness involving observed

probabilities so only a specific class of states and measurements can be self-tested within this regime. More recently, there was another idea of DI tests concerning the full attainable range of the input-output correlations [21–23]. This provides the possibility of directly inferring the information of the measurement from the range [24] rather than certifying a targeted witness.

In this Letter, we propose and realize quantum detector self-characterization (QDSC), capable of characterizing general unknown quantum measurements, based fully on the detector outcomes of the measurement device itself, which thus can break the loop paradox in characterizing quantum systems. The idea is to retrieve the attainable region for measurement results in actual use of the detector,

$$\mathcal{W}(\pi) := \{[\text{Tr}(\rho\pi_0), \dots, \text{Tr}(\rho\pi_{n-1})] | \rho \geq 0, \text{Tr}(\rho) = 1\},$$

termed as the response range of a quantum measurement. The response range can be formalized as the expectation values of a set of operators and derived by the fundamental constraints on quantum systems and uncertainty relations [25]. Distinguished from conventional QDT which explicitly involves probe states, this procedure [conceptually shown in Fig. 1(b)] reconstructs the measurement directly from the statistics of measurement outcomes $\{p^{(j)}\}$ without knowing which states are measured. With practical data in finite statistics, the problem is recast into an optimization problem that aims at giving a best estimation of the range $\mathcal{W}(\pi)$ consistent with the data, that is,

$$\begin{aligned} & \min \mathcal{F}[\mathcal{W}(\pi), \{p^{(j)}\}], \\ & \text{subject to } \pi_k \geq 0 \quad \text{and} \quad \sum_k \pi_k = I, \end{aligned} \quad (2)$$

where $\mathcal{F}[\mathcal{W}(\pi), \{p^{(j)}\}]$ is a cost function evaluating how well data fit the estimation. From the estimated range $\mathcal{W}(\pi)$ one can recover the information about the POVM without involving the density matrices of states. Compared with self-calibrating tomography [9,10] that combines measurement statistics and *a priori* knowledge in states or measurement operators to perform a joint tomography, the self-characterization method directly analyzes the collective behaviors of the measurement results mapped from the entire state space rather than certain set of states.

To apply this QDSC method to the characterization of practical devices, we implemented two representative measurements for tomography purpose, mutually unbiased bases (MUB) and symmetric informationally complete (SIC) measurements for single-qubit system [26], with photonic setups shown in Fig. 2. These two measurements are of particular interests in quantum information applications [32,33]. The experimental setup consists of two parts: state preparation (a) and measurement (b) or (c). The state preparation starts with a heralded single photon source via spontaneous parametric down-conversion. A polarizing beam splitter and three electronically controlled wave plates prepare probe states $\{\rho^{(j)}\}$ encoded in the polarization degree of freedom of single photons. The states are sent to a measurement apparatus with operations on the polarization modes and spatial modes on the single photons and detection with photon-counting detectors. The clicks of each detector correspond to an outcome π_k of the

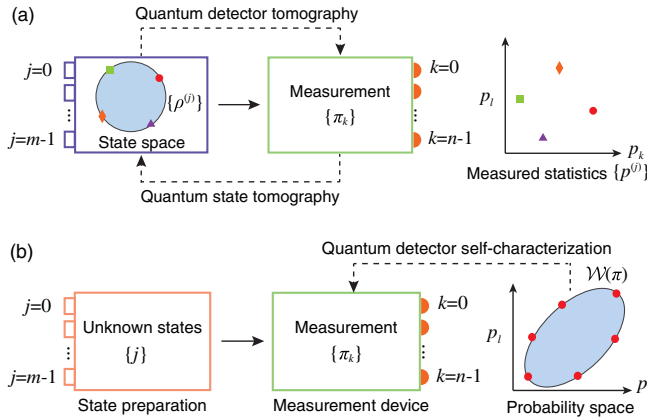


FIG. 1. Schematic diagram of quantum tomography and self-characterization. (a) Tomography of quantum measurements demands a set of known probe states, whereas tomography of quantum states demands well-calibrated quantum detectors. This forms a loop paradox in calibrating quantum systems. (b) In contrast, quantum detector self-characterization only uses the detector outcome probabilities from the measurement part itself to reconstruct the response range of the measurement, with unknown states, which thus can break the aforementioned loop paradox.

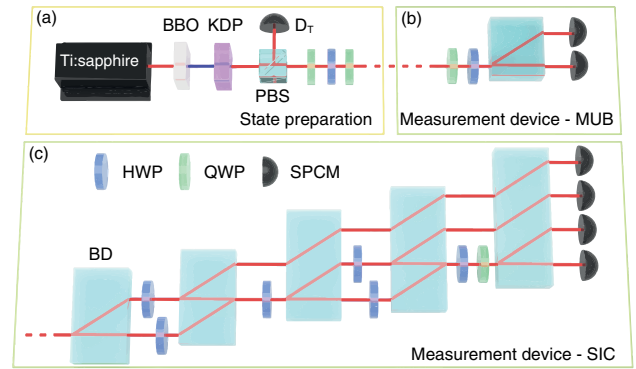


FIG. 2. Experimental setup. (a) Heralded single photons are generated via spontaneous parametric down-conversion, followed which a set of probe states are prepared by three electronically controlled wave plates and directed towards the measurement device (b) or (c). (b) The MUB device is composed of two wave plates followed by a beam displacer (BD) to perform projection on a certain basis. (c) The SIC device is a four-outcome general measurement realized by wave plates, BDs and single photon counting modules (SPCMs). BBO, β -barium borate crystal; KDP, potassium di-hydrogen phosphate; HWP, half wave plate; QWP, quarter wave plate.

measurement. For both measurements, we collected the measured statistics of detectors for 50 probe states sampled on the Bloch sphere [26]. Note although QDSC does not need to know the exact form of probe states, we recorded the settings of state preparation for the following tomographic reconstruction.

For qubit measurements used in our experiment, it has been shown [21] that the response range $\mathcal{W}(\pi)$ is a set $\{p\}$ satisfying

$$\mathcal{L} = (p - t)^T Q^+ (p - t) \leq 1, \quad (3)$$

and p is subject to $(I - QQ^+)(p - t) = 0$ which is equivalent to the requirement of linear dependencies among outcomes of the POVM [see the Supplemental Material [26] for a derivation of Eq. (3)]. The matrix Q and the vector t are given by $Q_{k,l} = \text{Tr}(\pi_k \pi_l)/2 - \text{Tr}(\pi_k)\text{Tr}(\pi_l)/4$ and $t_k = \text{Tr}(\pi_k)/2$, and $(\cdot)^+$ denotes the Moore-Penrose pseudoinverse. More precisely, the matrix Q quantifies the overlap of POVM elements and the vector t represents the weight of POVM elements, thus Q and t identify the POVM $\{\pi_k\}$ up to the equivalence class of unitary operations and relabeling of outcomes [26]. The physical constraint $\pi_k \geq 0$ can be written as $t_k^2 - Q_{k,k} \geq 0$ in the Q, t representation. Geometrically, the inequality is in a center form of an n -dimensional (hyper)ellipsoid centered on t . Upon considering the linear dependencies of the POVM elements, Eq. (3) may reduce to an ellipsoid, an ellipse, or a segment depending on the number of linear independent operators in $\{\pi_k\}$.

The characterization in our experiment is based on several assumptions: (i) the dimension of the system (qubit system in our case), and (ii) the probe states are adequately sampled to cover the boundary of the state space. In this sense our method is semi device independent. In addition, we assume fair sampling, i.e., the registered statistics is a representative sample of the generated states and the state preparation and measurement device are uncorrelated. These requirements are reasonable for an optical experiment and not more than a standard tomography scenario. The characterization procedure firstly extracts features in the data set via singular value decomposition and principle component analysis. This step removes the redundant linear dependent outcomes and is robust against experimental noise (see the Supplemental Material for details [26]). Then we perform a convex hull of the processed data to obtain the boundary data set \mathcal{B} . In the estimation we resort to the direct least squares between the boundary of the estimated range and the boundary data $[1 - (p^{(j)} - t)^T Q^+ (p^{(j)} - t)]^2$ for $j \in \mathcal{B}$ as the cost function. As a result, the characterization is conducted with only the measured statistics by solving the constrained optimization problem

$$\begin{aligned} \min \sum_{j \in \mathcal{B}} [1 - (p^{(j)} - t)^T Q^+ (p^{(j)} - t)]^2, \\ \text{subject to } t_k^2 - Q_{k,k} \geq 0. \end{aligned} \quad (4)$$

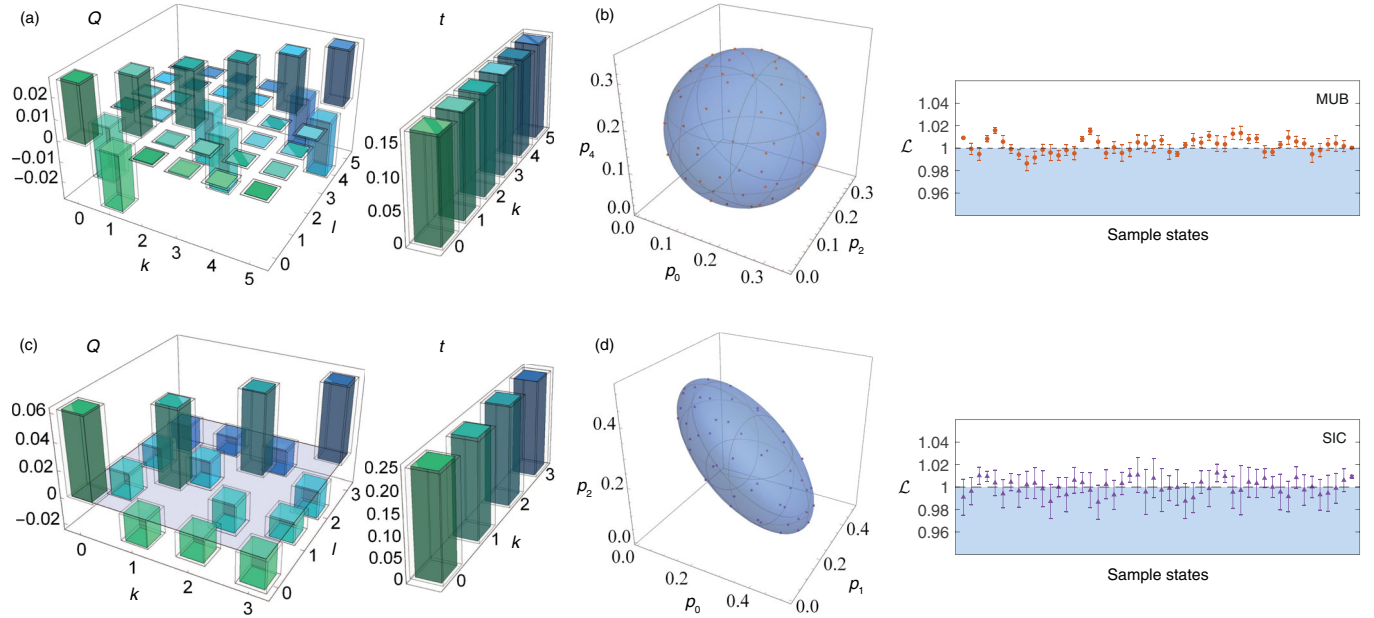


FIG. 3. Results of quantum detector self-characterization (QDSC). (a), (c) The reconstructed Q and t (chromatic bars) for the MUB and SIC devices, respectively. The corresponding results of quantum detector tomography (transparent bars with solid line edges) are also plotted for comparison. (b), (d) Left: the estimated response range (blue region) and the measured data (points), illustrated in the probability space despite the linear dependencies of the measurement operators, for the MUB and SIC devices, respectively. Right: the detailed results represented in terms of the values of \mathcal{L} in Eq. (3). Error bars are standard uncertainties derived from 40 runs of the experiment.

Figure 3 shows the experimental results of QDSC of the two measurements. To show the performance of self-characterization, we also give the results reconstructed with conventional QDT (with the same probe states) for comparison. In the QDT scenario, we use the measured statistics $\{p^{(j)}\}$, combined with the density matrices $\{\rho^{(j)}\}$ derived by the settings of wave plates, to numerically solve the convex optimization problem in Eq. (1) and reconstruct the POVM elements $\{\pi_k\}$ (thereby Q^{tom} and t^{tom}). The reconstructed results Q^{sc} and t^{sc} via QDSC are in well agreements with the reconstruction by conventional QDT [see Figs. 3(a) and 3(c)], having the fidelities $F_Q = [\text{Tr}(\sqrt{Q^{\text{tom}}Q^{\text{sc}}}\sqrt{Q^{\text{tom}}})]^2 / [\text{Tr}(Q^{\text{tom}})\text{Tr}(Q^{\text{sc}})]$ and $F_t = (\sum_k \sqrt{t_k^{\text{tom}}t_k^{\text{sc}}})^2$ above 99.99% with the tomographic reconstruction (QDT) for both implementations [26]. To further visualize the results of the QDSC, we plot the reconstructed response range together with the measured data in Figs. 3(b) and 3(d). The response range and the

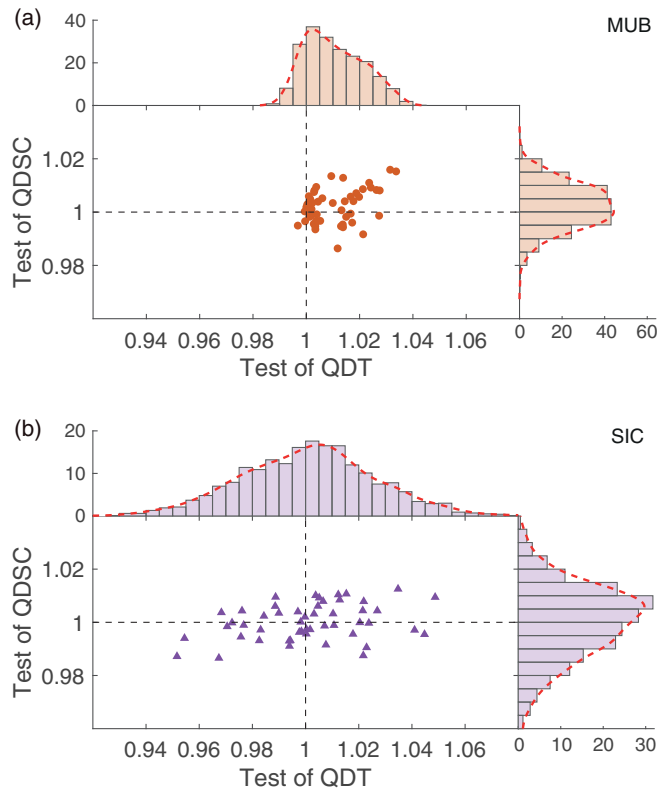


FIG. 4. Comparison of quantum detector tomography (QDT) and self-characterization (QDSC). The results are represented via tests of (a) the MUB device (red dot) and (b) the SIC device (purple triangle). Each marker represents the measured values of \mathcal{L} in Eq. (3) averaged over 40 runs for a same probe state. The marginal distributions in the horizontal (QDT) and vertical (QDSC) axes, represented by histograms from the 50×40 data before average and the corresponding Kernel fittings (red dashed lines), reflect the deviations of the measured data from the bound (black dashed lines).

measured data are illustrated in a three-dimensional probability space of its linear independent outcomes, despite the linear dependent ones (due to the fact that $p_k + p_{k+1} = 1/3$ for $k = 0, 2, 4$ for the MUB device and $\sum_k p_k = 1$ for the SIC device).

The comparison of QDT and QDSC in terms of the distribution of \mathcal{L} is shown in Fig. 4. The distribution reflects how well the range of the reconstruction fits the observed data, therefore giving a DI verification of the reconstructions. It can be seen from the results that the QDSC shows less violations of Eq. (3) in average compared with QDT. In contrast with QDT which suffers from the errors in state preparation, the QDSC method is solely based on the measured statistics that is completely accessible at the detection side, thus is more robust to experimental imperfections in state preparation. The deviations from the bound in the results of QDSC are mainly attributed to the statistical fluctuations on the measurement results.

The quantities Q and t represent the overlap between different elements of the POVM and the trace of each element, respectively, which fully characterizes the structure of the POVM, i.e., the physical model of the measurement device [34]. The representation given by QDSC is up to symmetry transformations that can be understood as the transformation of the reference frame of the whole system [35,36]. The reference frame can be specified with respect to the measurement POVM, then further usage of the measurement device can be conducted in a consistent way. To validate the usefulness of QDSC and demonstrate the break of the circular argument, we in turn perform a state tomography with the measurement calibrated by QDSC, and compare the results with those calibrated by QDT and those without *a priori* calibration (see Fig. S2 of the Supplemental Material [26]).

In conclusion, we realize quantum detector self-characterization that solely utilizes the events produced in the measurement part to explore the geometrical structure of the detector response. We have applied the self-characterization method to two typical, extensively used measurements, highlighting its feasibility and robustness in practical cases. The present self-characterization method extends witness-based methods to a range-based method in characterizing quantum systems and devices. Together with a modeling on the response range of measurement operators, this method can be further generalized to more complicated devices. Future works will investigate the range for high-dimensional systems and entangled states. We expect the range-based techniques will become a new means for specifying quantum systems and mapping detector response [37], and find their applications in a wide range of quantum information tasks such as cryptography, random number generation [19] and metrology, especially where calibrating measuring apparatus is required in advance.

The authors thank M. Dall'Arno, F. Buscemi, B. Zeng, X. Ma, P. Zeng, Z. Hradil, L. L. Sánchez-Soto, and N. Yu for enlightening discussions. This work was supported by the National Key Research and Development Program of China (Grant No. 2017YFA0303703) and National Natural Science Foundation of China (Grants No. 91836303, No. 61975077, No. 61490711, and No. 11690032).

*phyvv@nus.edu.sg

†lijian.zhang@nju.edu.cn

‡A. Z and J. X contributed equally to this work.

- [1] E. Knill, R. Laflamme, and G. J. Milburn, A scheme for efficient quantum computation with linear optics, *Nature (London)* **409**, 46 (2001).
- [2] P. Kok, W. J. Munro, K. Nemoto, T. C. Ralph, J. P. Dowling, and G. J. Milburn, Linear optical quantum computing with photonic qubits, *Rev. Mod. Phys.* **79**, 135 (2007).
- [3] B. L. Higgins, D. W. Berry, S. D. Bartlett, H. M. Wiseman, and G. J. Pryde, Entanglement-free heisenberg-limited phase estimation, *Nature (London)* **450**, 393 (2007).
- [4] K. J. Resch, K. L. Pregnell, R. Prevedel, A. Gilchrist, G. J. Pryde, J. L. O'Brien, and A. G. White, Time-Reversal and Super-Resolving Phase Measurements, *Phys. Rev. Lett.* **98**, 223601 (2007).
- [5] A. Luis and L. L. Sánchez-Soto, Complete Characterization of Arbitrary Quantum Measurement Processes, *Phys. Rev. Lett.* **83**, 3573 (1999).
- [6] G. M. D'Ariano, L. Maccone, and P. L. Presti, Quantum Calibration of Measurement Instrumentation, *Phys. Rev. Lett.* **93**, 250407 (2004).
- [7] J. S. Lundeen, A. Feito, H. Coldenstrodt-Ronge, K. L. Pregnell, C. Silberhorn, T. C. Ralph, J. Eisert, M. B. Plenio, and I. A. Walmsley, Tomography of quantum detectors, *Nat. Phys.* **5**, 27 (2009).
- [8] L. Zhang, H. B. Coldenstrodt-Ronge, A. Datta, G. Puentes, J. S. Lundeen, X.-M. Jin, B. J. Smith, M. B. Plenio, and I. A. Walmsley, Mapping coherence in measurement via full quantum tomography of a hybrid optical detector, *Nat. Photonics* **6**, 364 (2012).
- [9] A. M. Brańczyk, D. H. Mahler, L. A. Rozema, A. Darabi, A. M. Steinberg, and D. F. V. James, Self-calibrating quantum state tomography, *New J. Phys.* **14**, 085003 (2012).
- [10] D. Mogilevtsev, J. Řeháček, and Z. Hradil, Self-calibration for self-consistent tomography, *New J. Phys.* **14**, 095001 (2012).
- [11] D. Mayers and A. Yao, Quantum cryptography with imperfect apparatus, in *Proceedings 39th Annual Symposium on Foundations of Computer Science (Cat. No. 98CB36280)* (IEEE, Palo Alto, 1998) pp. 503–509.
- [12] E. S. Gómez, S. Gómez, P. González, G. Cañas, J. F. Barra, A. Delgado, G. B. Xavier, A. Cabello, M. Kleinmann, T. Vértesi, and G. Lima, Device-Independent Certification of a Nonprojective Qubit Measurement, *Phys. Rev. Lett.* **117**, 260401 (2016).
- [13] W.-H. Zhang, G. Chen, X.-X. Peng, X.-J. Ye, P. Yin, Y. Xiao, Z.-B. Hou, Z.-D. Cheng, Y.-C. Wu, J.-S. Xu, C.-F. Li, and G.-C. Guo, Experimentally Robust Self-Testing for Bipartite and Tripartite Entangled States, *Phys. Rev. Lett.* **121**, 240402 (2018).
- [14] A. Tavakoli, J. Kaniewski, T. Vértesi, D. Rosset, and N. Brunner, Self-testing quantum states and measurements in the prepare-and-measure scenario, *Phys. Rev. A* **98**, 062307 (2018).
- [15] J. Ahrens, P. Badziąg, A. Cabello, and M. Bourennane, Experimental device-independent tests of classical and quantum dimensions, *Nat. Phys.* **8**, 592 (2012).
- [16] M. Hendrych, R. Gallego, M. Mićuda, N. Brunner, A. Acín, and J. P. Torres, Experimental estimation of the dimension of classical and quantum systems, *Nat. Phys.* **8**, 588 (2012).
- [17] T. Lunghi, J. B. Brask, C. C. W. Lim, Q. Lavigne, J. Bowles, A. Martin, H. Zbinden, and N. Brunner, Self-Testing Quantum Random Number Generator, *Phys. Rev. Lett.* **114**, 150501 (2015).
- [18] X. Ma, X. Yuan, Z. Cao, B. Qi, and Z. Zhang, Quantum random number generation, *npj Quantum Inf.* **2**, 16021 (2016).
- [19] J. B. Brask, A. Martin, W. Esposito, R. Houlmann, J. Bowles, H. Zbinden, and N. Brunner, Megahertz-Rate Semi-Device-Independent Quantum Random Number Generators Based on Unambiguous State Discrimination, *Phys. Rev. Applied* **7**, 054018 (2017).
- [20] B. W. Reichardt, F. Unger, and U. Vazirani, Classical command of quantum systems, *Nature (London)* **496**, 456 (2013).
- [21] M. Dall'Arno, S. Brandsen, F. Buscemi, and V. Vedral, Device-Independent Tests of Quantum Measurements, *Phys. Rev. Lett.* **118**, 250501 (2017).
- [22] M. Dall'Arno, S. Brandsen, and F. Buscemi, Device-independent tests of quantum channels, *Proc. R. Soc. A* **473**, 20160721 (2017).
- [23] I. Agresti, D. Poderini, G. Carvacho, L. Sarra, R. Chaves, F. Buscemi, M. Dall'Arno, and F. Sciarrino, Experimental semi-device-independent tests of quantum channels, *Quantum Sci. Technol.* **4**, 035004 (2019).
- [24] M. Dall'Arno, F. Buscemi, A. Bisio, and A. Tosini, Data-driven inference, reconstruction, and observational completeness of quantum devices, [arXiv:1812.08470v2](https://arxiv.org/abs/1812.08470v2).
- [25] A. Sehwat, Deriving quantum constraints and tight uncertainty relations, [arXiv:1706.09319v2](https://arxiv.org/abs/1706.09319v2).
- [26] See the Supplemental Material at <http://link.aps.org/supplemental/10.1103/PhysRevLett.124.040402> for the experimental details, the derivation of Eq. (3), the self-characterization procedure, the detailed experimental results, and the results of state tomography with calibrated measurements, which includes Refs. [27–31].
- [27] J. M. Renes, R. Blume-Kohout, A. J. Scott, and C. M. Caves, Symmetric informationally complete quantum measurements, *J. Math. Phys. (N.Y.)* **45**, 2171 (2004).
- [28] P. Kurzyński and A. Wójcik, Quantum Walk as a Generalized Measuring Device, *Phys. Rev. Lett.* **110**, 200404 (2013).
- [29] Z. Bian, J. Li, H. Qin, X. Zhan, R. Zhang, B. C. Sanders, and P. Xue, Realization of Single-Qubit Positive-Operator-Valued Measurement via a One-Dimensional Photonic Quantum Walk, *Phys. Rev. Lett.* **114**, 203602 (2015).
- [30] Y.-y. Zhao, N.-k. Yu, P. Kurzyński, G.-y. Xiang, C.-F. Li, and G.-C. Guo, Experimental realization of generalized

- qubit measurements based on quantum walks, *Phys. Rev. A* **91**, 042101 (2015).
- [31] J. Chen, Z. Ji, C.-K. Li, Y.-T. Poon, Y. Shen, N. Yu, B. Zeng, and D. Zhou, Discontinuity of maximum entropy inference and quantum phase transitions, *New J. Phys.* **17**, 083019 (2015).
- [32] W. K. Wootters and B. D. Fields, Optimal state-determination by mutually unbiased measurements, *Ann. Phys. (Leipzig)* **191**, 363 (1989).
- [33] J. Řeháček, B.-G. Englert, and D. Kaszlikowski, Minimal qubit tomography, *Phys. Rev. A* **70**, 052321 (2004).
- [34] H. Ren and Y. Li, Modeling Quantum Devices and the Reconstruction of Physics in Practical Systems, *Phys. Rev. Lett.* **123**, 140405 (2019).
- [35] E. P. Wigner, *Group Theory and Its Application to the Quantum Mechanics of Atomic Spectra* (Academic Press, New York, 1959); translation from German by J. J. Griffin, *Gruppentheorie und ihre Anwendung auf die Quantenmechanik der Atomspektren (in German)* (Friedrich Vieweg und Sohn, Braunschweig, Germany, 1931), ASIN B000K1MPEI.
- [36] S. D. Bartlett, T. Rudolph, and R. W. Spekkens, Reference frames, superselection rules, and quantum information, *Rev. Mod. Phys.* **79**, 555 (2007).
- [37] M. Cooper, M. Karpiński, and B. J. Smith, Local mapping of detector response for reliable quantum state estimation, *Nat. Commun.* **5**, 4332 (2014).